

Claudemir L. do Lago
Carlos A. Neves
Dosil Pereira de Jesus
Heron D. T. da Silva
José G. A. Brito-Neto
José A. Fracassi da Silva*

Departamento de Química
Fundamental,
Instituto de Química,
Universidade de São Paulo

Microfluidic devices obtained by thermal toner transferring on glass substrate

A new process for the manufacture of microfluidic devices based on deposition of laser-printing toner on glass substrates is described. It is an alternative method to the toner on polyester film (toner-polyester) one, previously introduced. Commercial laser printers cannot print directly on glass, thus the toner must first be printed on a special paper and then transferred by heating under pressure to the glass surface. Although this procedure is more complex than the toner-polyester one, it can be repeated several times, yielding multiple toner layers. Even without special alignment equipment, up to four layers could be satisfactorily piled up. Characterization tests revealed that the toner-glass devices have similar behavior as toner-polyester ones regarding the toner layer porosity. The main advantages of the toner-glass technology are improved mechanical stability, possibility of multiple toner layers, augmented electroosmotic flow (EOF), and improved heat transfer. On the other hand, toner adhesion to glass is weaker than to polyester, which limits the device lifetime and usable liquid media. The measured EOF mobility ($3.5 \times 10^{-4} \text{ cm}^2 \cdot \text{V}^{-1} \cdot \text{s}^{-1}$ for pH 7) suggests that it is mainly determined by the glass surface, being little influenced by the toner walls. Microchip electrophoresis with contactless conductivity detection and photometric detection were implemented using toner-glass devices.

Keywords: Conductivity detection / Microchip / Microfabrication / Miniaturization / Toner

DOI 10.1002/elps.200406076

1 Introduction

Micrototal analysis systems (μ TAS) have revolutionized the field of analysis. There are several examples of such microsystems and the number of publications is still growing [1–3]. Initial efforts were focused onto silicon, glass, and quartz as substrate materials for the implementation of microsystems [4–7], mainly due to the availability of well-established microelectronics protocols. It was soon demonstrated that polymeric substrates could also be employed for the construction of microdevices, and a number of alternative techniques to work with these materials were described [8–10].

Recently, a new process for production of microfluidic devices based on laser printing was proposed [11]. Briefly, the desired layout is laser-printed on a poly(ethylene terephthalate) (PET) transparency sheet, which is laminated with another PET transparency sheet. The regions where toner is deposited (black in the original

layout) act as a spacer and adhesion layer for both transparency sheets and the clear regions (white in the original layout) form cavities and channels for microfluidic purposes. Single toner layer (STL) results in channels ca. 6 μm high, but if both sheets are printed with specular images, a double toner layer (DTL) of ca. 12 μm height can be obtained. Due to the toner granularity and printer resolution, only wide channels can be obtained. On the other hand, because of the flexibility of the PET film, wide channels tend to be deformed by the lamination process, yielding shallower channels, which eventually collapse. Thus, for practical uses, channel widths between 50 and 200 μm should be designed.

Even a simple screening of the literature will show that the devices produced by this toner-polyester process are not among the best definition ones, such as those obtained by photolithography and related processes [2, 3, 12, 13]. However, this process has remarkable advantages when one considers its cost, simplicity, and quickness of prototyping and production. In the present work, we describe a new process for production of devices using glass as substrate, which is based on the previous work, as it also uses toner as a structural layer. Since toner cannot be di-

Correspondence: Professor Dr. Claudemir L. do Lago, Av. Prof. Lineu Prestes 748, CEP 05508-900, São Paulo – SP, Brazil
E-mail: claudemi@iq.usp.br
Fax: +55-11-3091-3837

Abbreviations: dpi, dots per inch; **DTL**, double toner layer; **PET**, poly(ethylene terephthalate); **STL**, single toner layer

* Present address: Instituto de Química, Universidade Estadual de Campinas, Campinas, Brazil

rectly printed onto glass using a conventional laser printer, the toner is first printed onto a special paper and then transferred by heating. This process was used to produce a number of devices for its characterization and analytical application.

2 Materials and methods

2.1 Reagents and solutions

All reagents and solvents were of analytical grade or better and were used as received. Deionized water was produced by a Nanopure UV system (Barnstead, Dubuque, IA, USA).

2.2 Fabrication process

The main steps of the fabrication process are depicted in Fig. 1. The layouts were drawn on a computer using software CorelDraw 7.0 (Corel, Ottawa, Canada) on Windows 98 and Sketch 0.6.15 (<http://sketch.sourceforge.net/>) under the Debian-SID distribution of the GNU/Linux operating system. An HP LaserJet 1300 (Hewlett-Packard, Palo Alto, CA, USA) was used, operating at 1200 dots per inch (dpi) in the raster mode. Several devices are laser-printed on an A4 toner transfer sheet (Ferragini, São Carlos – SP, Brazil) commonly used for printed circuit

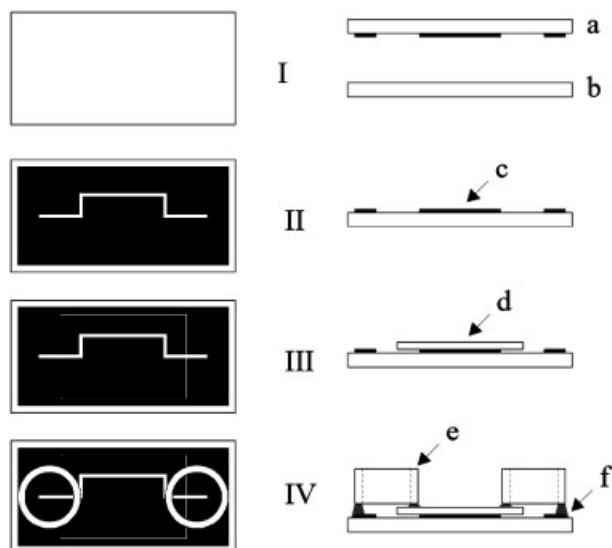


Figure 1. Diagram showing the four main steps of the microfabrication process. The left-hand column shows the top view and the right-hand one shows the side view. (I) Decal (a) is applied on the clean glass slide (b); (II) glass slide with the deposited toner layer (c); (III) cover glass (d) is welded, leaving the ends of the channel uncovered; (IV) reservoirs (e) are attached with glue (f).

board prototyping. This paper has a smooth and low-adherence surface, which allows the toner layer to be printed and later transferred to a higher affinity surface by heating. Similar results can be obtained by using waxed paper that remains after labels are removed from sheets for ink jet or laser printers [14]. The sheet is cut yielding several individual decals. The decal is positioned on a clean glass microscope slide ($26 \times 76 \times 1$ mm) (Glass Técnica, São Paulo – SP, Brazil) and then the toner layer is transferred to the glass surface by heating for 2 min at approximately 125°C under pressure (0.1–0.2 MPa). A heating press HT2020 (Ferragini) was used. This press has two metallic plates (the heating is developed in the upper plate), but the devices are positioned between two 5 mm thick silicone-rubber slabs, which equalize the pressure being applied to the glass pieces. Since it allows pressure adjustment without reading feedback, the optimal adjustment was empirically obtained. If two or more layers are desired, the heating and pressing step is repeated with new decals. For these additional steps, lining up of the toner layouts is critical. This lining up is done with naked eye by fixing the new decal on a base with the toner layer facing up and then positioning the slide with the toner layer facing down. The slide is also fixed with adhesive tape and the whole arrangement is pressed. After depositing the structural toner layers, a $150\ \mu\text{m}$ thick cover glass (GlassTécnica) is welded above them in order to seal the microchannels. This is done using the same hot press operated under the same conditions as the ones used for the toner transfer. The size of the cover glass depends on the layout of the device. The channels can be accessed at the edge of the cover glass or by drilling a hole through it [15]. Solution reservoirs were formed by gluing 5 mm long and 8 mm OD tubes made of poly(vinyl chloride) (PVC) at the channel entrances with bicomponent epoxy glue, as shown in Fig. 1. Special care must be taken at the sealing step to prevent the channel entrance from being closed when the cover glass is welded onto the toner layer. In this work, another cover glass, equal in thickness to the one being welded, was placed right next to it at the channel entrance region in order to equalize the pressure being applied on the toner layer, thus preventing it from being dented by the cover glass edge. This additional cover glass is easily removed after sealing by lifting it by its border, without damaging the toner layer.

2.3 Chemical resistance test

In order to evaluate the adhesion and chemical resistance, decals with the patterns from Fig. 2 were applied on several glass slides, which were submitted to the following aqueous solutions for several hours: H_3PO_4 (pH 2),

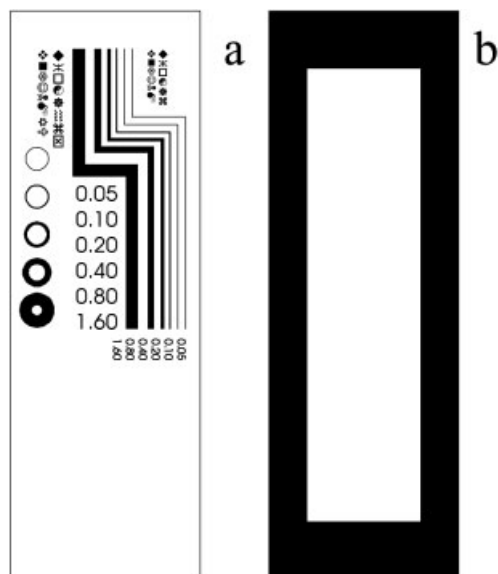


Figure 2. Layouts used in the chemical resistance essays. Layout is used to (a) test detachment of parts; (b) detect leakage. A cover glass is welded on the slides with the layout (b). Each layout is 25×75 mm.

NaOH (pH 12), 20% v/v methanol, 20% v/v acetonitrile, sodium dodecyl sulfate (SDS) in phosphate buffer (pH 7), and SDS in borate buffer (pH 9). The pattern from Fig. 2b was used to evaluate leakage through large toner barriers. In this case, cover glasses were welded. Two sets of slides were essayed at room temperature and at 60°C , being visually inspected after 2 and 24 h.

2.4 Electrical and dimensional characterization

Several single and multiple toner layer devices were built with different channel geometries and filled with 1 M KCl solution. An impedance analyzer HP 4194A (Hewlett-Packard) was used to evaluate cross-talking effect between parallel channels and channel depth. For the cross-talking evaluation, devices with two 10 mm long and $200\ \mu\text{m}$ wide parallel channels separated by 50, 100, 200, and $400\ \mu\text{m}$ wide toner barriers were analyzed in the range from 100 Hz to 5 MHz. To evaluate the possible ceiling deformation for wide channels (similar to the polyester film [11]), devices with 50, 100, 200, 400, 800, and $1600\ \mu\text{m}$ wide STL and DTL channels were used. The impedance measurements were also used to estimate channel depth of devices with 1–5 toner layers. The channel depths were determined considering the channel length equal to 24.0 ± 0.1 mm, the conductivity of the KCl solution equal to $111.31 \times 10^{-7}\ \Omega^{-1}\cdot\text{cm}^{-1}$ at 25°C , and the impedance is measured at 1 kHz. The effective channel widths were estimated by using an optical microscope

and a graduated scale. Similar toner-glass and toner-polyester devices were used for a comparative test of Joule heating effect. A straight 60 mm long and $200\ \mu\text{m}$ wide channel was filled with 20 mM phosphate buffer (pH 7) and increasing voltages were successively applied. The toner-polyester device was made following the procedure described elsewhere [11] and then fixed on a glass slide.

2.5 Electroosmotic flow

The device used for EOF measurements has the typical layout of an electrophoresis microchip, comprising a double-T injector in a $200\ \mu\text{m}$ wide separation channel with a total length of 60 mm. Two 1 mm wide copper strips with a gap of 1 mm between them were positioned at 44 mm downstream from the injection point and used for contactless conductivity detection at 600 kHz and $2\ V_{\text{peak-to-peak}}$ [11]. The electronic circuit of the detector as well as the high-voltage power supply were described elsewhere [16,17]. The channels were initially filled with 20 mM phosphate buffer (pH 7). The sample reservoir was filled with deionized water, which was electrokinetically injected for 3 s at 1.0 kV. The running voltage was 1.0 kV, resulting in an electric field of $170\ \text{V}\cdot\text{cm}^{-1}$. The EOF was calculated through the average migration time of the negative peak corresponding to the water plug in six consecutive runs.

2.6 Microchip electrophoresis

Two electrophoresis systems were implemented: one with conductivity detection and another with photometric detection. The microchip layout used for electrophoresis experiments was the same as the one used for EOF measurements. Figure 3 shows the electric diagram of the

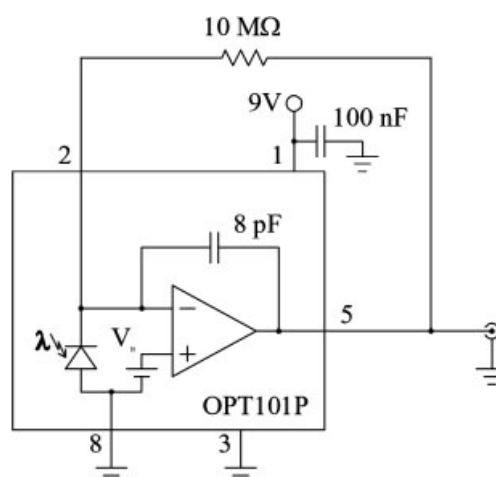


Figure 3. Electronic diagram of the photometric detector. The power supply is a 9 V battery.

photoelectric detector, which was adapted to a Q 709T-PL trinocular microscope (Quimis, Diadema-SP, Brazil) with a 100× objective. The illumination was done by a red light-emitting diode (LED) operating at 10 mA positioned directly below the condenser. The CE chip was implemented on a 76 × 26 mm glass slide and thus no adaptation was necessary to hold it in the microscope. The microscope objective was positioned at 40 mm downstream from the injection point, directly above the separation channel. The conductivity detection system is the same as the one used for the EOF measurements, except for the fact that the function generator was operated at 530 kHz with 2 V_{peak-to-peak}. The data acquisition was done by a software described elsewhere [16,17]. The sample rate was 6.5 samples/s. In order to measure the molar absorptivity of methylene blue, an HP 8452A (Hewlett-Packard) diode array spectrophotometer was used with a 2.5 mm optical length cuvette.

3 Results and discussion

3.1 Fabrication process

The substitution of the PET film by the glass slide renders a more complex process, because a toner transfer step is necessary. However, this may be advantageous if one needs a deeper channel, which can be obtained by the deposition of multiple toner layers. The practical limits of this multilayer approach will be discussed later, but some *a priori* features can be anticipated. Alignment of the successive decals is a critical step, because the positioning errors are cumulative, which excessively deforms the channels after some steps. On the other hand, hollows in one toner layer may be eliminated in some extent by a new layer. This occurs because, although the laser beam defines the regions that will receive toner, the image is not absolutely transferred to the substrate (paper or other film), *i.e.*, toner is randomly deposited on small regions. This feature can be easily observed in the microscope. The number of small hollows in the toner layer (caused by misprint or failure in the transfer step) is dramatically reduced after application of a second layer. The border of the channel is also improved, becoming better defined. Of course, these regions remain somewhat problematic, because of their porosity.

3.2 Dimensional, electrical, and chemical characterization

Table 1 shows the estimated channel depth as a function of its width. The standard deviation was estimated by error propagation and, for narrow channels, the dominant

Table 1. Channel depths for different channel widths^{a)}

| Nominal width ^{b)} (μm) | STL channel depth (μm) | DTL channel depth (μm) |
|----------------------------------|--------------------------|--------------------------|
| 100 | 11 ± 3 11 ± 3 | – |
| 200 | 7.5 ± 0.8 9 ± 1 | 13 ± 2 14 ± 2 |
| 400 | 8.8 ± 0.6 7.6 ± 0.5 | 14.5 ± 1.3 14.2 ± 1.2 |
| 800 | 10.1 ± 0.3 10.8 ± 0.3 | 17.1 ± 0.9 17.4 ± 0.9 |
| 1600 | 7.8 ± 0.4 8.3 ± 0.5 | 14.6 ± 1.5 14.2 ± 1.4 |

a) Two devices were evaluated for each nominal width

b) Width specified in the drawing software

error is exactly the one related to the channel width measurement. However, the trend of sustainment of channel depth is clearly observed for STL and DTL devices; in opposition to the results obtained for the toner-polyester technology [11]. In that case, the PET film is deformed by heating and pressurization, which does not occur with the glass slide and cover. Although the thin glass cover is flexible, its initial shape is restored after the sealing process. This is an interesting feature that can be explored when wide channels are desired, such as in microchip for free-flow electrophoresis [18–20].

Table 2 shows the estimated channel depth as a function of the number of toner layers for 200 and 400 μm width. Four layers is the practical limit. The results for five layers and width of 200 μm were not included, because the channels were often clogged. For 400 μm width, the channels are not clogged, but their internal geometry is severely modified (Fig. 4). There are two main reasons for this behavior: (i) accumulated errors in alignment and (ii) excessive flow of material (polymer from the toner composition) after several heating and pressing cycles. Therefore, alignment and pressing should be optimized if deep channels are desired.

The results of the cross-talking tests show a similar behavior as observed for the toner-polyester devices [11]: toner barriers thinner than 200 μm are not enough to prevent liquid flow between neighbor channels. These results suggest that the flexibility of the substrate (glass or PET) is not the most important factor to prevent cross-talking between neighbor channels. The compactness of the toner layer can be improved by extending the heating and pressing step or even by depositing successive layers. However, as shown before, these approaches can lead to

Table 2. Channel depths for different numbers of toner layers

| Number of toner layers | Depth for 200 μm nominal width channel ^(a) (μm) | Depth for 400 μm nominal width channel ^(a) (μm) |
|------------------------|--|--|
| 1 | 9.5 \pm 0.8 8.4 \pm 0.7 | 7.8 \pm 0.4 7.8 \pm 0.4 |
| 2 | 19.8 \pm 1.7 15.6 \pm 1.3 | 13.8 \pm 0.8 13.1 \pm 0.8 |
| 3 | 19.4 \pm 1.6 22.7 \pm 1.9 | 18.3 \pm 1.2 18.5 \pm 1.2 |
| 4 | 25 \pm 2 25 \pm 2 | 21.9 \pm 1.6 19.3 \pm 1.3 |
| 5 | – | 17.1 \pm 1.1 18.7 \pm 1.2 |

a) For each number of layers, two devices were evaluated

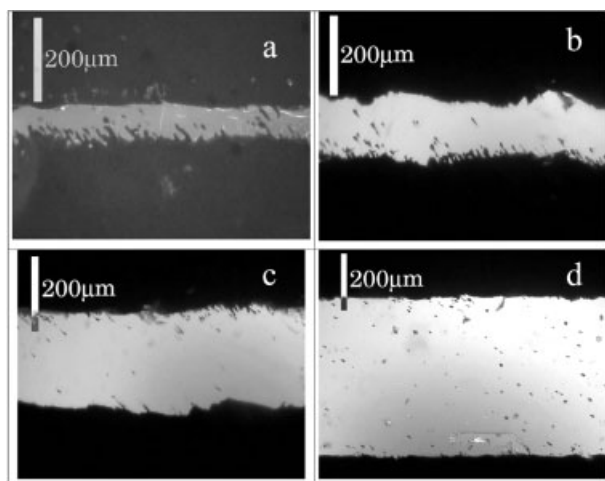


Figure 4. Optical microscope images of STL devices containing channels with nominal width of (a) 100; (b) 200; (c) 400; and (d) 800 μm .

shapeless channels. Thus, there is a balance between effectiveness of the toner barriers and the shape of the channels.

In the previous work [11], a 600 dpi printer was used. This new study was done with a 1200 dpi printer. Although a better definition of the printed patterns is observable at microscope, the final devices have similar properties as the 600 dpi ones. This similarity is probably due to the grain size of the toner particles. The measured EOF mobility was $3.5 \times 10^{-4} \text{ cm}^2 \cdot \text{V}^{-1} \cdot \text{s}^{-1}$ for pH 7, which is in good agreement with the expected values for silica and glass at that pH. Toner-polyester devices have EOF ca.

four times smaller, depending on the previous treatment. This is an advantage over toner-polyester when high EOF is desired.

The short-term exposition to the aqueous solution did not cause toner detachment or leakage at either temperature. However, long exposition proved deleterious in some cases. Surfactant (SDS, pH 7 and 9) solutions completely removed the patterns from the slides after 24 h. Thus, when the toner-glass devices are used for micellar electrokinetic chromatography (MEKC), they should not be exposed to the running electrolyte for a long period. On the other hand, these results suggest that aqueous surfactant solution can be effective in the recycling of the slides.

The exposition for 24 h to H_3PO_4 (pH 2) and NaOH (pH 12) solutions resulted in leakage through the toner layer, although it was not removed. Acetonitrile (20%) often caused leakage and pattern detachment. Methanol (20%) was the only medium that did not cause any deleterious effect to the devices even after 24 h exposition. These tests with aqueous solutions demonstrated that the affinity of the toner for the glass surface is smaller than that for PET. In fact, toner composition is optimized to have good adhesion on paper and transparency films and not necessarily on glass. The tests as a whole also suggest that the devices should not be exposed to any aqueous electrolyte for several hours.

Figure 5 shows the current as a function of the electric field for both toner-glass and toner-polyester. For low electric field, the current in the toner-polyester device was smaller than that in the toner-glass one. This may be due to the deformation of the PET film, which is expected to occur in some extent for a 200 μm wide channel [11]. The shapes of the curves show that glass is a better substrate

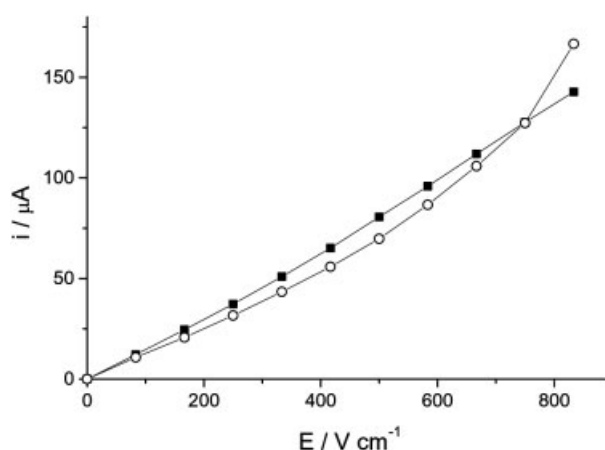


Figure 5. Current as a function of the electric field for both toner-glass (solid square) and toner-polyester (open circle).

than PET. There are two main causes: difference in thermal conductivities and substrate thickness. The thermal conductivity of the glass is greater than the one for PET: $0.15\text{--}0.4\text{ W}\cdot\text{m}^{-1}\cdot\text{K}^{-1}$ for PET (http://www.coolingelectronics.com/html/2001_may_techdata.html) and $0.75\text{--}1.2\text{ W}\cdot\text{m}^{-1}\cdot\text{K}^{-1}$ for soda-lime glasses [21]. The cover thickness has the same magnitude for both devices ($100\text{ }\mu\text{m}$ for PET film and $150\text{ }\mu\text{m}$ for glass), but the substrate thickness is quite different. In fact, since the toner-polyester device is fixed on glass, the first $100\text{ }\mu\text{m}$ layer is quite different, but the material is the same from that point on. However, the thermal contact is not perfect, generating a thin isolation layer of air.

3.3 Microchip electrophoresis

The integrated circuit OPT101P (Texas Instruments, Dallas, TX, USA) comprises a large-area photodiode (5.2 mm^2) and a transimpedance amplifier, with a sensitivity of $4 \times 10^6\text{ V/W}$ at 660 nm when a $10\text{ M}\Omega$ resistor is used in the loop. Taking into account the voltage level at the circuit output, the estimated light power on the detection point is ca. $1\text{ }\mu\text{W}$, resulting in a power density of $32\text{ }\mu\text{W}/\text{mm}^2$ for a 0.031 mm^2 field of vision. The internal 8 pF capacitance and the $10\text{ M}\Omega$ feedback resistor lead to a bandwidth of 1.8 kHz , which is appropriate to CE microchip detection. The output voltage is related to the light intensity at the detector and should be converted to absorbance, which was done by software. This software conversion is advantageous, because it simplifies the electronics.

Figure 6a shows steady-state measurements of absorbance for a continuous flow of water, 0.1 , 0.5 , and 1 mM methylene blue in a DTL toner-glass microchip. The molar absorptivity of the dye at 660 nm ($\epsilon = 4.3 \times 10^3\text{ m}^2\cdot\text{mol}^{-1}$) was measured in a 2.5 mm cuvette filled with 0.1 mM solution. The values of the molar absorptivity and absorbance of 0.1 mM solution inside the microdevice allow one to calculate the optical path length, which is equal to the channel depth. The depth calculated through this procedure is equal to $10.6 \pm 0.5\text{ }\mu\text{m}$, which is compatible with the results obtained through the impedance measurements. Figure 6b shows the applicability of the toner-glass device for electrophoresis through the electropherogram of a 1 mM methylene blue solution electrokinetically injected at 2 kV for 12 s (through the double-T injector). The electrokinetic injection accounts for the field amplification effect that makes the absorbance at the peak top greater than the one for steady-state condition. There are probably three causes for the asymmetry of the peak: (i) difference of mobilities between methylene blue and sodium from the running buffer; (ii) adsorption; and (iii) diffusion from the sampling channels during the run.

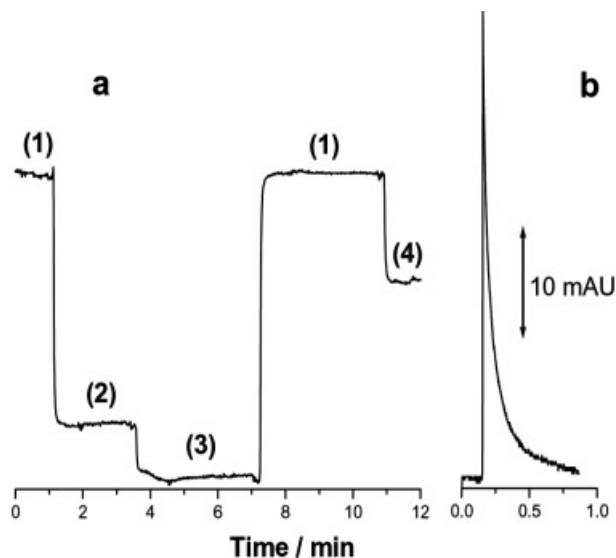


Figure 6. Absorbance response of methylene blue under electrophoretic and steady-state conditions. (a) Channel hydrodynamically filled with methylene blue in the concentration of (1) 1 mM ; (2) 0.1 mM ; (3) zero (deionized water); (4) 0.5 mM . (b) Electrophoretic migration of 1 mM methylene blue in sodium borate 20 mM running buffer ($\text{pH } 9.2$); detector positioned at 40 mm from injection point; electrokinetic injection at 2 kV for 12 s . The absorbance scale is the same for both plots.

Figure 7 shows an electropherogram of a sample containing KCl , NaCl , and LiCl $200\text{ }\mu\text{M}$ in each salt. The running buffer was 30 mM histidine/lactic acid in $9:1\text{ v/v}$ water:methanol. The sample was injected directly into the separation channel by applying 2.0 kV for 5 s at the sample reservoir. Although the concentrations of all analytes are the same, the corresponding signal intensities are different. The response factor for potassium is higher than the one for sodium, which is higher than the one for lithium. This is the expected trend, which is due to the different mobilities of the ions. First, the conductivity detector sensitivity is proportional to the ion mobility. Second, electrokinetic injection causes a bias towards higher-mobility species. The result is similar to the one for the toner-polyester device [11]. The main difference is that the EOF is much higher for the glass devices than for the polyester ones, thus, using the same running buffer, the resolution was poorer. The histidine/lactic acid buffer with methanol added reduces the EOF and improves the resolution [22]. The baseline for toner-glass as well as for toner-polyester drifts in a greater extent than is observed in the electropherograms obtained with conventional CE with contactless conductivity detector [16, 17, 22]. This observation is probably related to the better heat exchange efficiency of the silica capillary in a convective and temperature-controlled air bath.

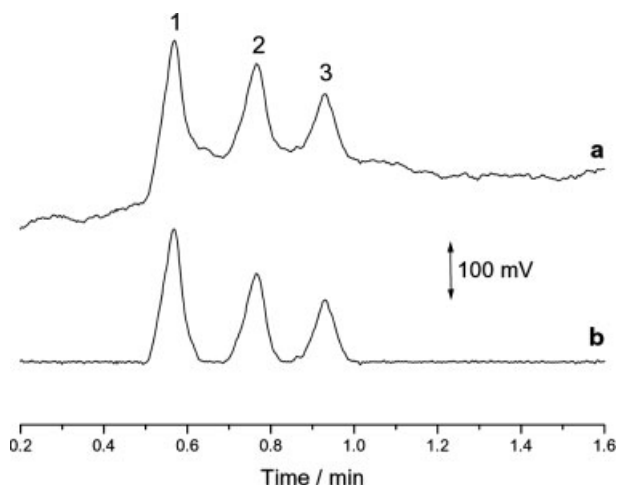


Figure 7. Electropherograms (a) before and (b) after baseline correction of a 200 μM solution of K^+ (1), Na^+ (2), and Li^+ (3). Running buffer was 30 mM histidine/lactic acid in 9:1 (v/v) water:methanol; electrokinetic injection at 2.0 kV for 5 s; separation voltage was 1 kV; contactless conductivity detection at 530 kHz and 2.0 $V_{\text{peak-to-peak}}$. Baseline correction was done in Origin 5.0 (Microcal, Northampton, MA, USA).

A rigorous comparison between the sensitivities of the contactless conductivity detector on PET and glass is not possible, because of the differences in running buffer, sample injection and channel shape. However, one can note that although the cover glass is 50% thicker than the PET film, its dielectric constant is greater (3–4 for polyesters [21] and 7.75 for soda-lime glass; <http://www.valleydesign.com/sodalime.htm>). Thus, similar results are obtained.

4 Concluding remarks

Electrolytes containing surfactants should be avoided, because of the lower adhesion of toner on glass. This suggests that toner composition or glass surface should be modified to improve the adhesion on glass in order to make the devices chemically resistant, such as the toner-polyester ones, which withstand the same conditions for weeks. On the other hand, the glass pieces can be easily recycled. There are other pros and cons of this new process when compared to the toner-polyester technology. Although toner-polyester remains the simplest way to produce microfluidic devices, toner-glass technology has four basic advantages: (i) improved mechanical stability, (ii) possibility of multiple toner layers, (iii) augmented EOF,

and (iv) improved heat transfer. Both technologies have a similar feature: it is possible to make microfluidic devices through a dry process with a minimum of chemical residues.

This work was supported by Fundação de Amparo à Pesquisa do Estado de São Paulo (FAPESP). Authors thank FAPESP and Conselho Nacional de Desenvolvimento Científico e Tecnológico (CNPq) for the fellowships, Texas Instruments for the OPT101P samples, and Dr. Z. G. Richter for the English revision.

Received May 14, 2004

5 References

- [1] Erickson, D., Li, D. Q., *Anal. Chim. Acta* 2004, 507, 11–26.
- [2] Reyes, D. R., Iossifidis, D., Auroux, P.-A., Manz, A., *Anal. Chem.* 2002, 74, 2623–2636.
- [3] Auroux, P.-A., Iossifidis, D., Reyes, D. R., Manz, A., *Anal. Chem.* 2002, 74, 2637–2652.
- [4] Manz, A., Graber, N., Widmer, H. M., *Sens. Actuators B* 1990, 1, 244–248.
- [5] Manz, A., Miyahara, Y., Miura, J., Watanabe, Y., Miyagi, H., Sato, K., *Sens. Actuators B* 1990, 1, 249–255.
- [6] Manz, A., Harrison, D. J., Verpoorte, E. M. J., Fettingter, J. C., Paulus, A., Ludi, H., Widmer, H. M., *J. Chromatogr.* 1992, 593, 253–258.
- [7] Jacobson, S. C., Moore, A. W., Ramsey, J. M., *Anal. Chem.* 1995, 67, 2059–2063.
- [8] Rossier, J., Reymond, F., Michel, P. E., *Electrophoresis* 2002, 23, 858–867.
- [9] McDonald, J. C., Duffy, D. C., Anderson, J. R., Chiu, D. T., Wu, H. K., Schueller, O. J. A., Whitesides, G. M., *Electrophoresis* 2000, 21, 27–40.
- [10] Becker, H., Gartner, C., *Electrophoresis* 2000, 21, 12–26.
- [11] Lago, C. L., Silva, H. D. T., Neves, C. A., Brito-Neto, J. G. A., Silva, J. A. F., *Anal. Chem.* 2003, 75, 3853–3858.
- [12] Manz, A., *Chimia* 1996, 50, 140–143.
- [13] Kutter, J., *Trends Anal. Chem.* 2000, 19, 352–363.
- [14] Daniel, D., Gutz, I. G. R., *Electrochem. Commun.* 2003, 5, 782–786.
- [15] Silva, H. D. T., Lago, C. L., *Química Nova* 2003, 26, 278–280.
- [16] Fracassi da Silva, J. A., do Lago, C. L., *Anal. Chem.* 1998, 70, 4339–4343.
- [17] Fracassi da Silva, J. A., Guzman, N., do Lago, C. L., *J. Chromatogr. A* 2002, 942, 249–258.
- [18] Roman, M. C., Brown, P. R., *Anal. Chem.* 1994, 66, 86A–94A.
- [19] Poggel, M., Melin, T., *Electrophoresis* 2001, 22, 1008–1015.
- [20] Zhang, C.-X., Manz, A., *Anal. Chem.* 2003, 75, 5759–5766.
- [21] Silva, J. A. F., Ricelli, N. L., Carvalho, A. Z., Lago, C. L., *J. Braz. Chem. Soc.* 2003, 14, 265–268.
- [22] Weast, R. C., *CRC Handbook of Chemistry and Physics*, CRC Press, Boca Raton, FL 1990.